PHYSICAL REVIEW B **93**, 140410(R) (2016)

Doppler effect in a solid medium: Spin wave emission by a precessing domain wall drifting in spin current

Hong Xia,[1,2] Jie Chen,[1,2] Xiaoyan Zeng,[3] and Ming Yan[1,2,*]
[1]*Department of Physics, Shanghai University, Shanghai 200444, China*
[2]*Shanghai Key Laboratory of High Temperature Superconductors, Shanghai 200444, China*
[3]*Department of Mathematics, Shanghai University, Shanghai 200444, China*
(Received 26 January 2016; revised manuscript received 8 April 2016; published 20 April 2016)

The Doppler effect is a fundamental physical phenomenon observed for waves propagating in vacuum or various media, commonly gaseous or liquid. Here, we report on the occurrence of a Doppler effect in a solid medium. Instead of a real object, a topological soliton, i.e., a magnetic domain wall (DW) traveling in a current-carrying ferromagnetic nanowire, plays the role of the moving wave source. The Larmor precession of the DW in an external field stimulates emission of monochromatic spin waves (SWs) during its motion, which show a significant Doppler effect, comparable to the acoustic one of a train whistle. This process involves two prominent spin-transfer-torque effects simultaneously, the current-driven DW motion and the current-induced SW Doppler shift. The latter gives rise to an interesting feature, i.e., the observed SW Doppler effect appears resulting from a stationary source and a moving observer, contrary to the laboratory frame.

DOI: 10.1103/PhysRevB.93.140410

The Doppler effect (DE) refers to a frequency shift of a wave caused by the relative motion between the wave source and the observer. One example from everyday experience is the rise (drop) in pitch of a train siren when the train approaches (recedes). Another well-known example is the redshift/blueshift of lights emitted by a moving source. Technologies based on DE have been widely used in astronomy [1,2], weather forecast [3,4], medical diagnosis [5], satellite communication [6], etc. In nature, DE is universal for waves of any type. We here describe a DE for spin waves (SWs) propagating in ferromagnets, with the wave source served by a naturally formed magnetic structure, a domain wall (DW), traveling inside the sample.

The relevant process involves multiple spin-transfer-torque (STT) effects [7–10]. Electrons passing through ferromagnetic samples become spin polarized, thus generating a spin current which carries spin angular momentum. Conversely, a spin current reacts on the local magnetization of noncollinear spin configurations by exerting a STT. In recent years, STT has attracted much attention because it provides an alternative way to manipulate the magnetization and therefore may have important applications in spintronics [11–19]. Generally speaking, STT can induce various physical effects, depending on the experimental setup. One example of particular interest is the current-driven DW motion in magnetic nanowires, which has been exploited for the development of the racetrack memory [19]. Moreover, STT can also act on SWs, the collective excitations of the magnetization. The standard expression of the in-plane STT consists of two terms, the adiabatic [20,21] and nonadiabatic ones [22,23]. The adiabatic STT causes a modification of the SW dispersion relation [24–26], referred as the current-induced SW Doppler shift, which provides a quantitative measurement of the spin current [25]. Despite its name, this effect "should not be confused with a true Doppler shift" [25], which is the subject of this Rapid Communication. The nonadiabatic STT, on the other hand, affects the SW amplitude, offering an experimental approach to determine the nonadiabatic STT parameter β [27], which is crucial for STT-induced magnetization dynamics [22,28].

The STT effects on DWs and SWs both play a part in affecting the SW emission from a current-driven DW. First, the DW motion causes a normal Doppler shift to the SW frequency and wavelength. Meanwhile, the current alters the SW dispersion relation, or, equivalently, causes an effective flow of the magnetic medium [25,26]. In our particular setup, the DW travels with a speed just equal to the flow rate of the magnetic medium, which is thus analogous to a boat drifting downstream in a river, as schematically illustrated in Fig. 1. Consequently, the actual SW DE corresponds to the situation of a stationary source and a moving observer, yielding a shifted frequency but a constant wavelength. Concerning the nonadiabatic effect, the current can automatically pump energy into one branch of the emitted SWs, effectively reducing the SW attenuation.

SW emissions from a DW were reported in several previous studies [29–33], but the SW DE due to the DW motion has not been addressed. In this Rapid Communication, we explore SW emissions from a moving transverse DW formed in a cylindrical nanowire [Fig. 1(b)] [34], which clearly manifest this phenomenon. Driven by a current/field, the DW dynamics in such a geometry is characterized by a smooth spiraling motion along the wire, with the linear velocity predominantly determined by the current density and the angular velocity by the field strength [35,36]. The latter predetermines the fundamental frequency of SWs emitted by the DW. In an ideal case, i.e., if the wire possesses a perfect circular symmetry, the DW behaves as a "massless" object [35]. Its precession is energetically free, causing no disturbance to the magnetic medium and thus no SW excitation. For our very purpose, we exploit a slightly massive DW as a SW source by introducing a transverse anisotropy to break the circular symmetry of the system.

Using a code package MUMAX [37], we perform fully three-dimensional micromagnetic simulations by numerically

*Corresponding author: myan@shu.edu.cn

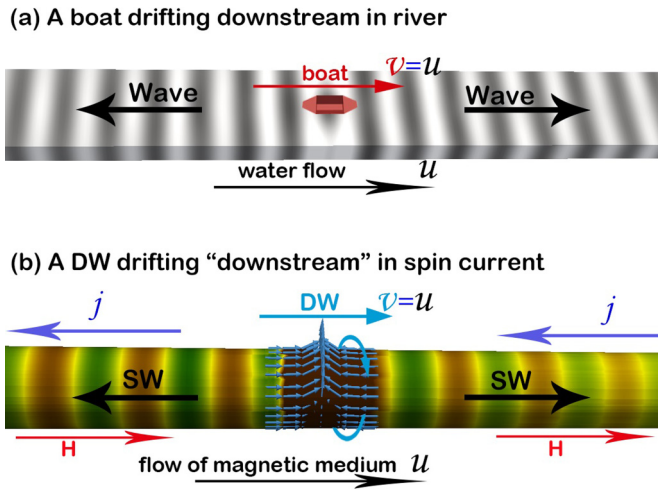

FIG. 1. (a) Schematic illustration of a boat beating the water surface with a constant frequency, thus generating water waves. The drift of the boat in the water flow causes Doppler shifts to the waves. (b) An analogous effect occurring in a magnetic nanowire of 10 nm diameter. The DW precession stimulates SW emissions while the DW drifting "downstream" in a spin current, arising from an electrical current flowing in opposite direction.

solving the extended Landau-Lifshitz-Gilbert equation with additional STT terms [22,23],

$$\frac{d\vec{m}}{dt} = \gamma \vec{H}_{\text{eff}} \times \vec{m} + \frac{\alpha}{M_s}\left[\vec{m} \times \frac{d\vec{m}}{dt}\right] - (\vec{u}\cdot\vec{\nabla})\vec{m} + \frac{\beta}{M_s}\vec{m} \times [(\vec{u}\cdot\vec{\nabla})\vec{m}], \quad (1)$$

where $\vec{m}$ is the normalized local magnetization, M_s the saturation magnetization, γ the gyromagnetic ratio, $\vec{H}_{\text{eff}}$ the effective field, and α the damping factor. The vector $\vec{u}$ is given by

$$\vec{u} = -\frac{g\mu_B P}{2eM_s}\vec{j}, \quad (2)$$

where $\vec{j}$ is the current density, g the Landé factor, μ_B the Bohr magneton, e the electron charge, and P the polarization rate of the current. Note that $\vec{u}$ has a unit of velocity, which defines the spin-current flow rate and the DW velocity in our case. The simulated wire is 4 μm long[1] and 10 nm in diameter with the material parameters typical for Permalloy ($M_s = 1$ T, exchange constant $A = 1.3\times10^{-11}$ J/m, $P = 0.7$, $\alpha = 0.01$, and anisotropy constant $K = 10^3$ J/m^3). The easy axis is vertical to the wire. In calculation, the wire is discretized into 1 nm $\times$1 nm $\times$1 nm cubic cells.[2]

[1]All the data about SWs are extracted before they reach the boundaries of the wire. Therefore, the results presented in this Rapid Communication should be considered as for an infinitely long wire.

[2]The accuracy of the discretization is confirmed by the agreement between the simulation and the analytical calculation assuming a perfect symmetry of the wire, which also indicates that a sample roughness can be tolerated to a certain extent.

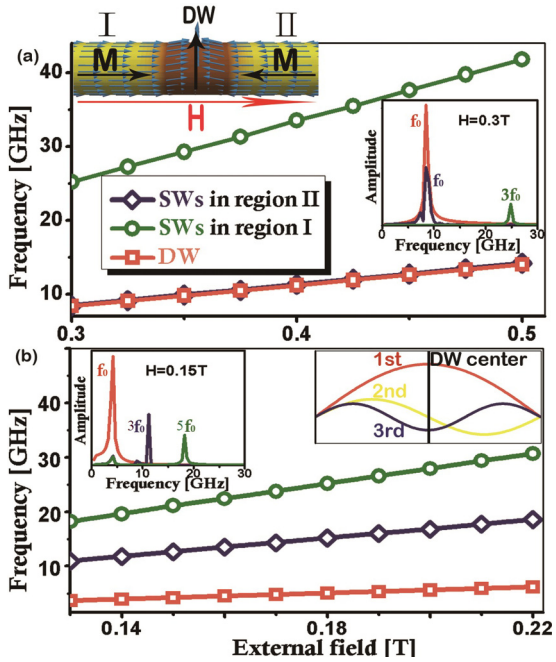

FIG. 2. Frequencies of the DW precession and SWs excited in two regions, indicated in the top inset, as functions of field plotted in two field ranges [(a) and (b)] separately. The lines are theoretical values of the Larmor frequency f_0 and its overtones. In a high field range (a), the SWs propagating in regions I and II are dominated by a SW mode with frequency $3f_0$ and f_0, respectively. In a low field range (b), the most prominent SW mode in regions I and II has frequency of $5f_0$ and $3f_0$, respectively. Fourier spectra of the dynamic magnetization at $H = 0.3$ and 0.15 T are plotted in the two insets. The Fourier amplitude is in arbitrary units. The right inset of (b) shows that the even-numbered harmonics are antisymmetric with respect to the DW center.

We first focus on the SW emission by a field-driven DW. The small anisotropy introduced in the system has little impact on the DW behavior. The DW simply precesses in the field with the Larmor frequency, similar as in an isotropic wire [35,36]. This is illustrated in Fig. 2, showing the match between the rotational frequency of the DW and the Larmor frequency. However, unlike the free rotation in a symmetric wire, the DW precession in an anisotropic wire causes periodic accumulation and dissipation of energy, thus provoking SW excitations in the system, as shown in Fig. 1(b) and a movie in the Supplemental Material [38]. The emitted SWs are analyzed by Fourier transformation of the dynamical magnetization, showing two characteristic features. First, the two SW branches emitted on different sides of the DW have a well-defined yet distinct frequency but an identical wavelength. Second, the SW frequencies show different field dependences in different field ranges. A summary of the SW frequency as a function of field is plotted in Fig. 2 consisting of two field ranges. These results coincide with a recently published work using a biaxial-chain model [33].

The emitted SW spectra are governed by the following constraints. First, the Larmor precession of the DW sets up a fundamental frequency, only allowing the SW mode with this frequency and its overtones to be excited. Furthermore,

the excitation of even-numbered harmonics is forbidden because of the mismatch between their waveforms with the DW precession, as illustrated in Fig. 2(b). Finally, the SW dispersion relation, which yields a cutoff frequency ω_c, serves as another filter for emitted SW modes. As a result, only odd-numbered harmonics with a frequency higher than ω_c can propagate in the wire. In the presence of an external field, the SW dispersion differs in two oppositely magnetized domains separated by the DW, leading to different ω_c and SW excitations. For brevity, we refer to the two domains with their local magnetization parallel and antiparallel to the field as regions I and II, respectively.

By neglecting the small transverse anisotropy of the wire, the SW dispersion relation can be derived as [39]

$$\omega = \gamma\left[\pm H + M_s\left(\tfrac{1}{2} + qk^2\right)\right], \tag{3}$$

where ω is the angular frequency, k the wave vector, q an exchange-dependent positive constant, and H the external field, which takes a positive (negative) sign in region I (II). From Eq. (3), the SW cutoff frequency $\omega_c = \omega(k = 0)$ at various H can be easily calculated. By comparing ω_c with the Larmor frequency $\omega_0 = \gamma H$, one can then determine the SW modes that can be excited. For example, at $H = 0.15$ T, one obtains $\omega_c = 0.35\gamma$ in region II, which is larger than ω_0 but smaller than $3\omega_0$. Therefore, the lowest-frequency odd-numbered harmonic that is allowed to propagate is the third one with $\omega = 3\omega_0$. Similarly, one can deduce the lowest-frequency mode in region II at $H = 0.3$ T to be the first harmonic. From Eq. (3), ω_c in region I is always larger than that in region II by $2\gamma H = 2\omega_0$. Therefore, the lowest-frequency modes in region I at $H = 0.15$ and 0.3 T must be the fifth and third harmonics, respectively. This analysis provides a quantitative explanation for the field dependence of the SW frequency obtained in simulations, as summarized in Fig. 2. As shown by the Fourier spectra at two fields (insets of Fig. 2), the SW emission is dominated by the lowest-frequency mode of all harmonics that are allowed to propagate, thus assuming a good monochromaticity. From Eq. (3), one also notices that the SWs excited in regions I and II at a given field must have the same wavelength, consistent with the simulation result.

Besides its precession, the field also drives the DW to propagate. Owing to the symmetry of the wire, the DW motion is solely attributed to the damping effect and its speed is proportional to α [35]. In the field range applied in this study, the corresponding DW speed is in the order of m/s or less, which is tiny in comparison with the SW propagating speed (several hundred m/s or above). Therefore, a DW driven only by a field can be considered as "stationary" as far as the SW DE is concerned.

In the following, we discuss the SW emission by a DW driven also by an electrical current. Similar to the field-driven case, the small mass introduced to the DW has no significant influence on the current-driven dynamics either. The dynamical property of a massless DW reported in Ref. [35] still applies to this massive one. On one hand, the DW rotation would be affected by the presence of the nonadiabatic STT, resulting in a frequency change proportional to $|\alpha - \beta|$ [36]. In the case of $\beta = \alpha$, as assumed at the moment, the DW precessional frequency remains unchanged. On the other hand, the DW propagation, mainly attributed to the adiabatic

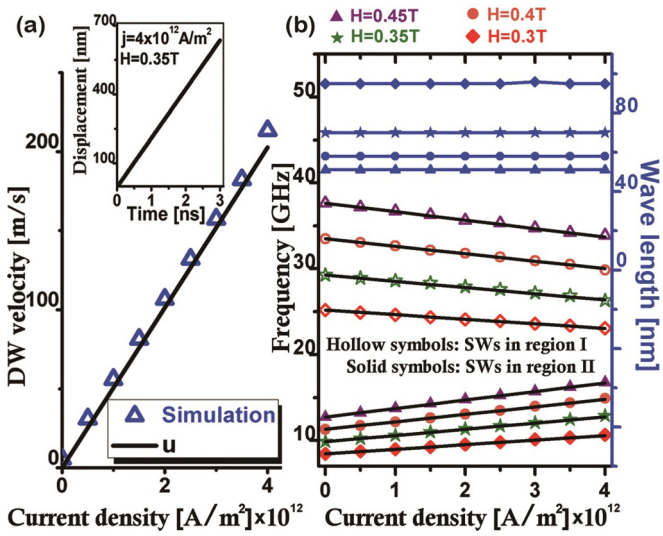

FIG. 3. (a) DW velocity as a function of current. Inset: DW displacement as a function of time driven by a particular current. (b) SW frequency (left label) and wavelength (right label) at various currents and fields. The black lines are theoretical values of SW frequency calculated from Eq. (6). The blue lines are just guides to the eye.

STT, acquires a velocity approximately equal to $\vec{u}$. This is demonstrated in Fig. 3(a), showing the simulation data of the current-driven DW motion. Compared to the field-driven case, the DW driven by a sufficiently large current can travel with a much higher speed, thus becoming a moving SW source. The emission of SWs by a fast-moving DW can be viewed in a movie in the Supplemental Material [38].

The current-induced high-speed DW motion gives rise to a sizable DE to the emitted SWs. For instance, at current density $j = 2\times10^{12}$ A/m^2, which is experimentally feasible [19], the DW speed u reaches about 100 m/s. The resulting Doppler shift to a SW mode with a propagation speed of about 1200 m/s can be estimated to be as significant as the acoustic one of a train whistle. Figure 3(b) summarizes the SW Doppler shifts observed in our simulations with varying currents. Here, we focus on a field range, which allows the excitation of the first and third harmonics in regions I and II, respectively. Since the DW moves from region I towards region II, the SWs in regions I and II are redshifted and blueshifted, respectively.

Besides the frequency, a normal DE due to a moving source also causes a shift to the wavelength. Our simulation, however, yields a constant SW wavelength showing no dependence on the DW velocity [Fig. 3(b)]. This discrepancy is attributed to another adiabatic STT effect, which causes a modification of the SW dispersion relation having the form [25]

$$\omega' = \omega(k) + \vec{u}\cdot\vec{k}, \tag{4}$$

where $\omega(k)$ is the SW dispersion with no current. Consider a SW mode propagating in region II, where the wave vector $\vec{k}$ is parallel to $\vec{u}$. Suppose it has an original frequency ω_0, wave vector k_0, and phase velocity v_0. If the SW source (DW) is moving with the velocity $\vec{u}$, the observed frequency of the SW

is then given by

$$\omega_1 = \frac{v_1}{v_1 - u}\omega_0, \tag{5}$$

where $v_1 = \omega_1/k_1$ is the observed transmission velocity of the SW and k_1 the observed wavelength. By recalling that ω_1 and k_1 satisfy Eq. (4), one easily proves $k_1 = k_0$, which is also true for the SWs propagating in region I.

There is a more intuitive understanding on this issue. As pointed out in Refs. [25,26], the current-induced SW dispersion change can be considered as resulting from a flow of the magnetic medium in which SWs propagate. In this picture, the SW source (DW) is stationary relative to the medium because its moving speed u is nothing but the effective flow rate of the medium. Consequently, the SW DE appears to be produced by a moving observer, which yields a constant wavelength and a frequency shift taking the form of

$$\omega_1 = \frac{v_0 + u}{v_0}\omega_0, \tag{6}$$

which is equivalent to Eq. (5). As shown in Fig. 3(b), the SW frequency shifts obtained in simulations at various currents are in perfect agreement with Eq. (6). Although $\beta = \alpha$ is assumed in the above calculation, we emphasize that the Doppler shift observed is a general effect, regardless of the value of β because of the independence of the DW velocity on β.[3]

Finally, we discuss the current effect on the SW amplitude. It has been shown in Ref. [27] that the nonadiabatic STT acts either against or in favor of the intrinsic damping, causing a weakened or enhanced SW attenuation depending on the relative direction between $\vec{k}$ and $\vec{u}$. In our case, this effect takes place on the two SW branches emitted by the DW simultaneously although in opposite ways, as shown in Fig. 4. For a clear demonstration, $\beta = 2\alpha$ is used in this calculation. It is worth mentioning that the amplitude of the SWs propagating in front of the DW with $\vec{k}$ parallel to $\vec{u}$ is amplified, which helps to sustain a long-lasting SW propagation. This is beneficial for applications based on propagating SWs.

In summary, we show that a massive DW precessing in a thin magnetic cylinder acts as a monochromatic SW source. When driven by an electrical current, the DW motion together with the altered SW dispersion result in a notable Doppler shift to the SW frequency but a constant wavelength. Persistent progresses in the fabrication of high-quality magnetic cylindrical nanowires [40,41] make it promising to conduct experimental investigations on this effect in the near future. From an application point of view, our work proposes a setup which can generate SWs with precise and tunable frequency. Compared to the ordinary method of exciting SWs in experiments, utilizing a precessing DW has an advantage of requiring only dc but no ac signals [29–33]. Furthermore, the DW can be freely relocated along the SW guide by a current pulse, thus serving as a mobile SW emitter. We also believe that our work, which reports on the DE of a moving topological soliton, could also be of interest to researchers in nonlinear physics.

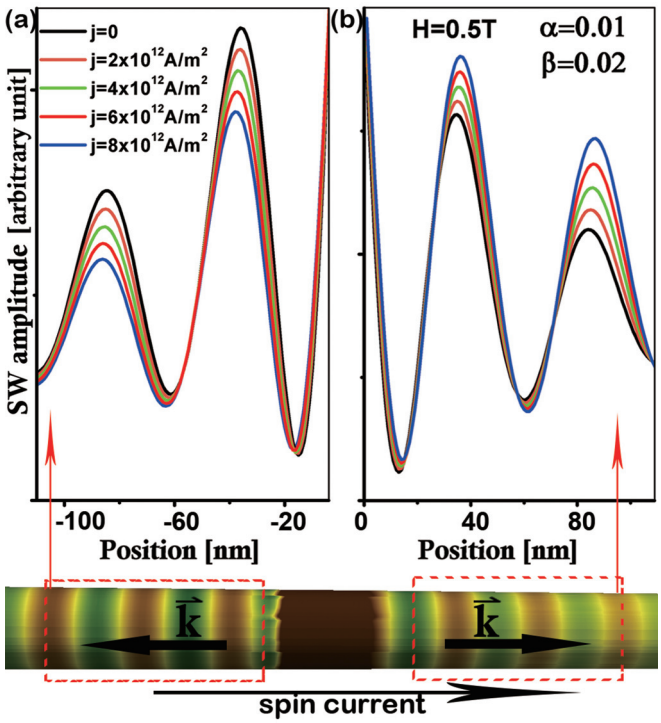

FIG. 4. Nonadiabatic STT effect on the SW amplitudes at various currents with $\beta = 2\alpha$. The SW curves are extracted from the average dynamic magnetization over the cross section of the wire within two regions [(a) and (b)] indicated by the red dashed line boxes.

[3]In the case of $\beta \neq \alpha$, the current would cause a frequency shift to the DW precession and thus to the excited SWs. It can be estimated that the magnitude of this additional shift with a moderate value of β is much smaller than the Doppler shift observed in this study.

This work is supported by the National Natural Science Foundation of China (No. 11374203) and Shanghai Key Laboratory of High Temperature Superconductors (No. 14DZ2260700).

[1] J. B. Rice, W. H. Wehlau, and V. L. Khokhlova, Astron. Astrophys. **208**, 179 (1989).
[2] M. C. Johnson, W. D. Cochran, A. C. Cameron, and D. Bayliss, Astrophy. J. Lett. **810**, 2 (2015).
[3] L. Armijo, J. Atmos. Sci. **26**, 570 (1969).
[4] *Radar in Meteorology: Battan Memorial and 40th Anniversary Radar Meteorology Conference*, edited by D. Atlas (American Meteorological Society, Boston, 1990).
[5] D. H. Evans and W. N. McDicken, *Doppler Ultrasound*, 2nd ed. (Wiley, New York, 2000).
[6] J. Mass and E. Vassy, Adv. Space Sci. Technol. **4**, 1 (1962).
[7] L. Berger, Phys. Rev. B **33**, 1572 (1986).
[8] L. Berger, J. Appl. Phys. **63**, 1663 (1988).
[9] J. C. Slonczewski, J. Magn. Magn. Mater. **159**, L1 (1996).
[10] L. Berger, Phys. Rev. B **54**, 9353 (1996).

[11] E. B. Myers, D. C. Ralph, J. A. Katine, R. N. Louie, and R. A. Buhrman, Science **285**, 867 (1999).
[12] B. Özyilmaz, A. D. Kent, D. Monsma, J. Z. Sun, M. J. Rooks, and R. H. Koch, Phys. Rev. Lett. **91**, 067203 (2003).
[13] S. Mangin, D. Ravelosona, J. A. Katine, M. J. Carey, B. D. Terris, and E. E. Fullerton, Nat. Mater. **5**, 210 (2006).
[14] M. Tsoi, A. G. M. Jansen, J. Bass, W.-C. Chiang, V. Tsoi, and P. Wyder, Nature (London) **406**, 46 (2000).
[15] S. I. Kiselev, J. C. Sankey, I. N. Krivorotov, N. C. Emley, R. J. Schoelkopf, R. A. Buhrman, and D. C. Ralph, Nature (London) **425**, 380 (2003).
[16] K.-J. Lee, A. Deac, O. Redon, J.-P. Noziéres, and B. Dieny, Nat. Mater. **3**, 877 (2004).
[17] A. Yamaguchi, T. Ono, S. Nasu, K. Miyake, K. Mibu, and T. Shinjo, Phys. Rev. Lett. **92**, 077205 (2004).
[18] E. Saitoh, H. Miyajima, T. Yamaoka, and G. Tatara, Nature (London) **432**, 203 (2004).
[19] S. S. P. Parkin, M. Hayashi, and L. Thomas, Science **320**, 190 (2008).
[20] G. Tatara and H. Kohno, Phys. Rev. Lett. **92**, 086601 (2004).
[21] Z. Li and S. Zhang, Phys. Rev. Lett. **92**, 207203 (2004).
[22] S. Zhang and Z. Li, Phys. Rev. Lett. **93**, 127204 (2004).
[23] A. Thiaville, Y. Nakatani, J. Miltat, and Y. Suzuki, Europhys. Lett. **69**, 990 (2005).
[24] J. Fernández-Rossier, M. Braun, A. S. Núñez, and A. H. MacDonald, Phys. Rev. B **69**, 174412 (2004).
[25] V. Vlaminck and M. Bailleul, Science **322**, 410 (2008).
[26] R. D. McMichael and M. D. Stiles, Science **322**, 386 (2008).
[27] S.-M. Seo, K.-J. Lee, H. Yang, and T. Ono, Phys. Rev. Lett. **102**, 147202 (2009).
[28] S. Lepadatu, M. C. Hickey, A. Potenza, H. Marchetto, T. R. Charlton, S. Langridge, S. S. Dhesi, and C. H. Marrows, Phys. Rev. B **79**, 094402 (2009).
[29] R. Wieser, U. Nowak, and K. D. Usadel, Phys. Rev. B **69**, 064401 (2004).
[30] J. He and S. Zhang, Appl. Phys. Lett. **90**, 142508 (2007).
[31] S. J. Hermsdoerfer, H. Schultheiss, C. Rausch, S. Schäfer, B. Leven, S.-K. Kim, and B. Hillebrands, Appl. Phys. Lett. **94**, 223510 (2009).
[32] E. Martinez, L. Torres, and L. Lopez-Diaz, Phys. Rev. B **83**, 174444 (2011).
[33] X. S. Wang and X. R. Wang, Phys. Rev. B **90**, 184415 (2014).
[34] R. Hertel, J. Magn. Magn. Mater. **249**, 251 (2002).
[35] M. Yan, A. Kákay, S. Gliga, and R. Hertel, Phys. Rev. Lett. **104**, 057201 (2010).
[36] M. Yan, A. Kákay, and R. Hertel, Phys. Rev. B **89**, 054415 (2014).
[37] A. Vansteenkiste and B. Van de Wiele, J. Magn. Magn. Mater. **323**, 2585 (2011).
[38] See Supplemental Material at http://link.aps.org/supplemental/10.1103/PhysRevB.93.140410 for a movie showing the excitation of SWs by a stationary and a moving DW, respectively.
[39] J. Chen, H. Xia, X. Y. Zeng, and M. Yan, Physica B **481**, 59 (2016).
[40] Y. Xiang, W. Lee, K. Nielsch, G. Abstreiter, and A. Fontcubertai Morral, Phys. Status Solidi RRL **2**, 59 (2008).
[41] I. Minguez-Bacho, S. Rodriguez-López, M. Vázquez, M. Hernández-Vélez, and K. Nielsch, Nanotechnology **25**, 145301 (2014).